Available online at www.sciencedirect.com
SCIENCE DIRECT®
Journal of Solid State Chemistry 177 (2004) 2685–2690
JOURNAL OF SOLID STATE CHEMISTRY
http://elsevier.com/locate/jssc

Structural studies of cerium tantalates

Stephen J. Skinner,* Helen M. Palmer, Edwin S. Raj, and John A. Kilner

Department of Materials, Royal School of Mines, Imperial College of Science, Technology and Medicine, Prince Consort Road, London SW7 2BP, UK

Received 26 November 2003; received in revised form 29 January 2004; accepted 4 April 2004

Abstract

Structural data obtained from neutron diffraction studies of some cerium tantalate phases are presented, including the first report of the high temperature structure of a $CeTaO_4$ phase, $Ce_{0.85}TaO_{3.84}$ deduced from in situ data recorded at 900°C in vacuum. It was found that this material transformed from the low temperature $LaTaO_4$ type phase to the orthorhombic $A2_1am$ structure reported here, with a unit cell of $a = 5.64062(2)$ Å, $b = 14.81609(6)$ Å and $c = 3.93482(1)$ Å. This data agrees well with the previously proposed structural transformations.

Keywords: $CeTaO_4$; Structure; Transformation; $A2_1am$; Neutron diffraction

1. Introduction

$CeTaO_{4+\delta}$ has received some attention recently because of its interesting, flexible oxygen stoichiometry and the significant number of phase transformations associated with both the oxygen stoichiometry and the temperature [1–3]. The recent work by Thompson et al. [2] and Drew et al. [3] highlighted the remarkable oxidation/reduction behavior of the $CeTaO_{4+\delta}$ materials and builds on previous studies by Santoro et al. [4], Roth et al. [5,6], Negas et al. [7] and Cava et al. [8]. Thompson et al. studied the $\delta = 0.17$ material in particular and found a superstructure exists for this stoichiometry and, further, that three distinct regimes exist (i) $0.5 > x > 0.48$, (ii) $0.17 > x > 0.06$ and (iii) $0.4 > x > 0.34$ for the $Ce^{III}_{1-2x}Ce^{IV}_{2x}TaO_{4+x}$ representation of the material. Drew et al. [3] and Cava and Roth [9] both refer to a high temperature orthorhombic phase but neither report on the crystal structure, with Cava and Roth [9] indicating that the structure is likely to be similar to that of the related $LaTaO_4$ phase. Santoro et al. [4] used neutron diffraction to investigate $CeTaO_4$, $CeNbO_4$ and $NdTaO_4$ but concentrated only on the stoichiometric material at room temperature.

Further, preliminary investigations were performed on the $\delta = 0.17$ material with a view to possible use as an oxide ion conductor [1] exploiting the scope for interstitial oxide ion incorporation. Studies employing AC impedance spectroscopy indicated that the total resistance was comparable with current solid electrolyte materials at low temperatures but that at higher temperatures electronic conduction was present degrading the potential use of the material as an electrolyte. Also the relatively low level of electronic conduction would discount the possible use of the $CeTaO_{4+\delta}$ materials as mixed conducting cathodes. However, with the report of oxygen excess in Scheelite type [10–14] and Zircon type [15] oxides it is possible that further optimisation of this material would be achievable. Indeed, a related phase, $CeNbO_4$, has been shown to adopt a stable tetragonal Scheelite type structure at temperatures >650°C [16] and possible solid solution formation and consequent stabilisation of this polymorph would be of significant interest.

2. Experimental

Samples of $CeTaO_4$ were prepared following the method of Thompson et al. [2]. Ta_2O_5 (Aldrich, 99%) and CeO_2 (Aldrich, 99.9%) were combined in an agate

*Corresponding author. Fax: +44-020-7584-3194.
E-mail address: s.skinner@ic.ac.uk (S.J. Skinner).

0022-4596/$ - see front matter © 2004 Elsevier Inc. All rights reserved.
doi:10.1016/j.jssc.2004.04.004

mortar and pestle and mixed under acetone to ensure good mixing of the oxides. The mixture was then allowed to air dry before being placed in an alumina crucible and heated to 1000°C for an initial period of 12 h before further heating to 1500°C for a period of 16 h. Once the heating period was complete the sample was rapidly quenched to room temperature and plunged in to H_2O to prevent the formation of the $CeTa_3O_9$ and CeO_2 phases. It was also found that using the same starting materials and heating at 1500°C for 15 h under Ar would achieve the same results without the need for a quenching step. Further samples with oxygen excess concentrations were produced with a stoichiometry of up to $CeTaO_{4.17}$ through a single step synthesis involving the direct combination of the starting oxides. These were heated for 12 h in air at 1500°C before being cooled to air. No reoxidation step, as previously described [2,3], was necessary when using this preparative route.

Initial phase characterisation studies were performed by X-ray powder diffraction using a Phillips PW1700 series diffractometer with Cu$K\alpha$ radiation and secondary graphite crystal monochromator to confirm that single phase products had been produced. Further studies of the products were then undertaken at the neutron diffraction spallation source, ISIS, at the Rutherford Appleton laboratories on the high resolution powder diffractometer, HRPD. These studies were carried out in both static air and vacuum conditions.

3. Results and discussion

3.1. $CeTaO_4$

Several data sets were collected in vacuum over the temperature range 25–900°C and subsequently refined using the Rietveld method using the GSAS software package [17]. Initial data were recorded from the stoichiometric material at room temperature in vacuum ($\sim 10^{-5}$ mbar) and refined to the previously suggested model of Santoro et al. [4] resulting in good agreement with that report, with refined lattice parameters of $a = 7.61918(5)$ Å, $b = 5.53111(4)$ Å, $c = 7.76758(4)$ Å and $\beta = 100.889(1)^\circ$. The final refined atomic data are given in Table 1. These measurements thus confirmed the earlier findings and indicated that the samples were of the appropriate room temperature monoclinic structure, space group $P2_1/c$, and hence enabled the study to proceed to a temperature above that at which the transition to an orthorhombic phase has been previously determined. Consequently data were collected in situ at temperatures up to 900°C in vacuum for the $CeTaO_4$ sample as this is considerably above the reported transition temperature on heating of 818°C [3].

After recording the initial data set at 25°C further data were collected every 100°C from 300–900°C and the resulting data found to refine to the previously reported $P2_1/c$ model at all temperatures up to and including 800°C. A typical refinement is presented in Fig. 1 with the associated atomic parameters given in Table 2. Refined lattice parameters for all compositions are given in Table 3 and show a steady increase with temperature, and that the maximum angle, β, of 101.63° was achieved at 800°C immediately prior to the previously suggested structural change.

Diffraction data recorded from the material in situ at 900°C were refined with a 10 term shifted Chebyshev background function with the model based on that of the isostructural $LaTaO_4$ [8] which adopts the $BaMnF_4$ structure with all atoms occupying the 4*a* positions in the non-standard space group $A2_1am$. The atomic coordinates chosen for the initial model were based on those derived by Cava and Roth [9] in the isostructural

Table 1
Refined atomic parameters for $CeTaO_4$ in vacuum at 25°C

	x	y	z	U_{iso}*100	Occup.	Mult.
Ce1	0.34471(33)	0.7727(4)	0.09754(28)	0.66*	1.012(10)	4
Ta1	0.16650(20)	0.26572(33)	0.30385(19)	−0.06*	0.994(6)	4
O1	0.16872(29)	0.15956(30)	0.05523(29)	0.77*	1.024(10)	4
O2	0.05373(28)	0.58562(31)	0.20586(27)	0.44*	0.978(9)	4
O3	0.38259(24)	0.48502(33)	0.33105(25)	−0.19*	0.936(8)	4
O4	0.33378(24)	0.00883(38)	0.36622(24)	0.52*	0.986(9)	4
	U_{11}	U_{22}	U_{33}	U_{12}	U_{13}	U_{23}
Ce1	1.24(16)	−0.69(14)	1.65(16)	−0.48(12)	0.82(10)	−0.16(11)
Ta1	0.15(9)	0.69(10)	−0.83(8)	0.16(7)	0.29(6)	0.19(7)
O1	1.30(14)	0.47(13)	0.64(13)	0.06(9)	0.38(8)	0.24(8)
O2	0.63(13)	−0.32(11)	1.18(15)	0.25(8)	0.63(9)	0.22(8)
O3	0.08(13)	−0.76(12)	0.32(13)	−0.25(9)	0.63(8)	0.11(8)
O4	0.79(12)	0.73(13)	0.32(14)	0.32(9)	0.76(9)	−0.26(9)

$R_p = 5.62\%$, $R_{wp} = 6.36\%$, $\chi^2 = 3.705$.

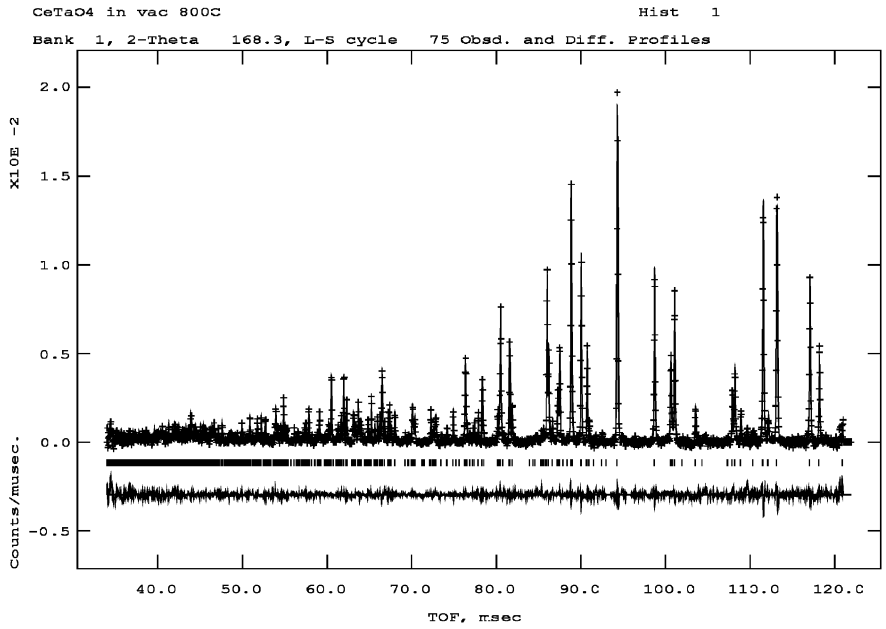

Fig. 1. Rietveld refinement of $CeTaO_4$ at 800°C in vacuum. Crosses represent experimental data, solid line is the fit with difference plot shown below.

Table 2
Refined atomic parameters for $CeTaO_4$ in vacuum at 800°C

Name	X	y	z	U_{iso}*100	Occup.	Mult.
Ce1	0.34143(31)	0.7711(4)	0.09635(27)	1.45*	1.008(10)	4
Ta2	0.16775(18)	0.26538(32)	0.30158(18)	1.02*	1.094(6)	4
O3	0.16816(33)	0.16685(30)	0.05083(27)	2.03*	1.033(10)	4
O4	0.05292(29)	0.58356(33)	0.21244(28)	2.28*	1.021(10)	4
O5	0.38134(23)	0.47997(36)	0.32989(24)	1.30*	1.013(9)	4
O6	0.33209(26)	0.00560(34)	0.36396(23)	1.86*	1.042(9)	4
Thermal parameters						
	U_{11}	U_{22}	U_{33}	U_{12}	U_{13}	U_{23}
Ce1	2.14(16)	1.28(15)	1.04(13)	−0.43(14)	0.49(10)	0.12(12)
Ta2	1.07(9)	0.83(10)	1.00(10)	−0.18(7)	−0.16(6)	0.02(6)
O3	3.36(15)	2.91(16)	0.14(12)	0.90(11)	0.79(9)	0.16(8)
O4	2.16(17)	1.76(14)	3.23(18)	1.03(9)	1.44(10)	0.54(10)
O5	0.85(13)	1.40(15)	1.49(13)	−0.39(9)	−0.10(9)	0.00(9)
O6	2.70(14)	1.29(14)	1.51(14)	0.66(10)	0.12(9)	0.10(9)

Table 3
Refined lattice parameters for the monoclinic $CeTaO_4$ phase from neutron diffraction data

Temp. (°C)	A	B	c	b
25	7.61919(5)	5.53113(3)	7.76757(4)	100.8891(5)
300	7.64054(5)	5.54669(4)	7.78717(5)	101.1615(6)
400	7.64273(4)	5.55355(3)	7.79204(4)	101.3039(5)
500	7.65359(4)	5.55957(3)	7.79510(3)	101.4639(4)
600	7.66061(4)	5.56647(3)	7.80186(3)	101.5593(4)
700	7.66772(3)	5.57241(2)	7.81491(3)	101.5497(4)
800	7.67473(3)	5.58127(2)	7.82329(2)	101.6350(3)

system discussed above. Refinement of the data indicated that the material was both Ce deficient and oxygen deficient (Table 4).

From the Rietveld refinement it was evident that under vacuum conditions there was a slight decomposition of the stoichiometric material to CeO_2 and a deficient cerium tantalate phase, $Ce_{1-x}TaO_{4-\delta}$ as peaks were observed in the neutron diffraction pattern that could be attributed to CeO_2. However a number of smaller peaks that could not be attributed to any CeO_2, Ta_2O_5 or related phases were also apparent, perhaps indicating that a superstructure phase was present. No evidence was found for the presence of the reported decomposition product, $CeTa_3O_9$ [2,3]. The refined lattice parameters for $Ce_{1-x}TaO_{4-\delta}$ were found to be $a = 5.64062(2)$ Å, $b = 14.81609(6)$ Å and $c = 3.93428(1)$ Å and the final refinement is presented in Fig. 2 with the final calculated bond distances given in

Table 4
Final refined atomic parameters for the orthorhombic phase, $Ce_{1-x}TaO_{4-\delta}$, in space group $A2_1am$

Name	X	y	z	U_{iso}*100	Occup.	Mult.
Ce1	0.1860(8)	0.16855(26)	0	2.31*	0.851(12)	4
Ta1	0.2237(4)	0.41515(12)	0	1.54*	1.000(6)	4
O1	0.4282(5)	0.30445(17)	0	1.77*	0.904(10)	4
O2	0.0605(4)	0.53012(18)	0	4.84*	0.994(14)	4
O3	0.4519(5)	0.66131(18)	0	2.82*	0.922(13)	4
O4	0.2454(8)	0.91395(29)	0	5.34*	0.920(10)	4

Thermal parameter

	U_{11}	U_{22}	U_{33}	U_{12}	U_{13}	U_{23}
Ce1	1.45(18)	4.38(24)	1.09(15)	−0.63(16)	0	0
Ta1	1.61(11)	1.81(10)	1.21(9)	0.28(9)	0	0
O1	0.86(15)	1.13(17)	3.32(17)	0.61(11)	0	0
O2	2.63(19)	3.15(21)	8.73(24)	1.07(17)	0	0
O3	2.43(20)	3.60(18)	2.43(17)	1.07(17)	0	0
O4	9.60(26)	6.41(19)	0.00(12)	0.30(22)	0	0

$R_p = 4.82\%$, $R_{wp} = 5.61\%$, $\chi^2 = 1.796$.

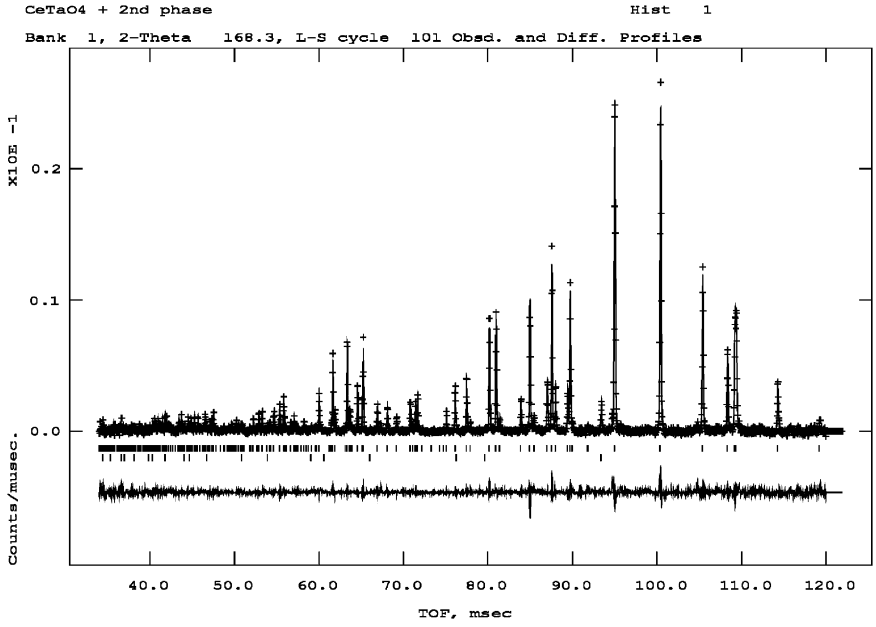

Fig. 2. Rietveld refinement of $CeTaO_4$ fitted to the orthorhombic $A2_1am$ model. Upper markers are $CeTaO_4$ phase, lower markers CeO_2 impurity. Crosses represent experimental data, solid line is the fit with difference plot shown below.

Table 5. These bond distances indicate that the Ta coordination environment consists of distorted octahedra of Ta–O bonds with a variation in bond length from 1.906 to 2.066 Å whilst the Ce is surrounded by 9 oxygen atoms at distances from 2.433 to 2.929 Å (Fig. 3).

The relationship between the orthorhombic and monoclinic cells is such that $a_o = b_m$, $b_o = \frac{1}{2}(4b_m + a_m)$ and $c_o = c_m$ [3,9] where the subscripts refer to the orthorhombic and monoclinic phases. Taking the lattice constants derived from the refinement of the stoichiometric material at room temperature we would expect that the high temperature orthorhombic phase would

Table 5
Refined Ce–O and Ta–O bond distances for $Ce_{1-x}TaO_{4-\delta}$ at 900°C

Bond	Length (Å)	Bond	Length (Å)
Ce–O1	2.433(5)	Ta–O1	2.005(3)
Ce–O1	2.479(3)	Ta–O2	1.936(3)
Ce–O1	2.479(3)	Ta–O2	2.066(3)
Ce–O2	2.929(4)	Ta–O3	1.906(3)
Ce–O2	2.929(4)	Ta–O4	1.971(1)
Ce–O3	2.846(5)	Ta–O4	1.971(1)
Ce–O3	2.476(4)		
Ce–O3	2.476(4)		
Ce–O4	2.770(4)		

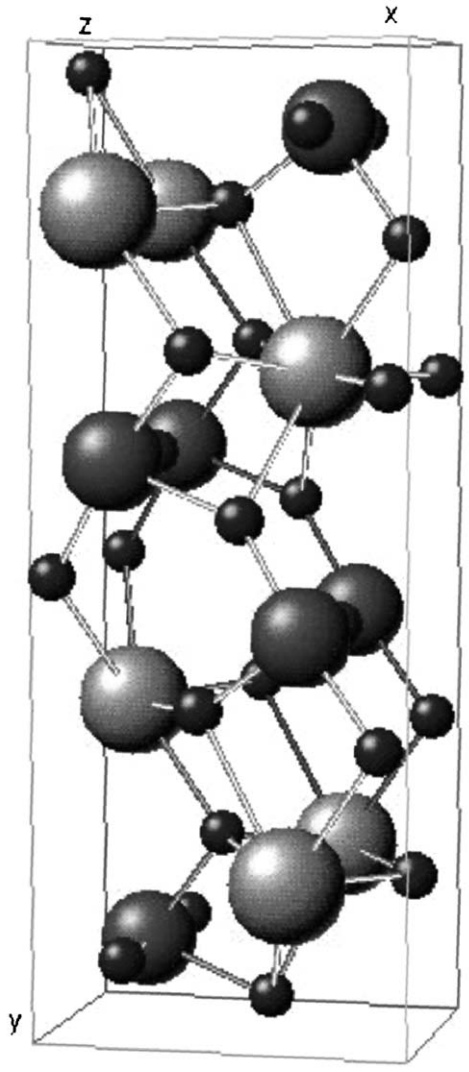

Fig. 3. Representation of the high temperature orthorhombic $CeTaO_4$ phase showing the coordination environments of the cations.

have the following lattice constants: $a = 5.531$ Å, $b = 14.946$ Å and $c = 3.883$ Å. It is clear that the experimentally determined lattice parameters are in reasonable agreement with these values and that the differences observed could be attributed to a combination of thermal expansion and the CeO_2 deficiency observed and the resulting non-stoichiometry reported.

Of further interest is the thermal anisotropy of all the refined atomic positions indicating significant thermal motion of all atomic positions in $Ce_{1-x}TaO_{4-\delta}$ at elevated temperatures. It was found that it was necessary to refine the thermal parameters of each atomic position anisotropically to allow convergence of the refinement and achievement of a physically plausible model. Using isotropic temperature factors resulted in temperature factors being unreasonably high and site fractions significantly greater than 1 for more than one site.

3.2. $CeTaO_{4+\delta}$

Neutron diffraction data were recorded from this complex material, with a δ-value close to 0.17, at room temperature in air and subsequently at temperatures up to 900°C. Close inspection of the diffraction data obtained for this material indicated that at temperatures of up to 900°C no phase transformation similar to that observed for the stoichiometric material had occurred. Further structural details were considered from the Reitveld refinement of the data recorded at 800°C. An initial model, based on the monoclinic crystal structure in the $P2_1/c$ space group detailed elsewhere [2], was used for a typical case, i.e. that of the data recorded at 800°C. It was apparent from the refinement of this data that the process of heating in air had, as expected, caused a

Table 6
Refined atomic parameters for $CeTaO_{4+\delta}$ at 800°C in air, spacegroup $P2_1/c$

	X	y	z	U_{iso}*100	Occup.	Mult.
Ce1	0.3487(5)	0.7725(8)	0.0941(5)	5.05*	1.085(19)	4
Ta1	0.16398(33)	0.2524(6)	0.29487(30)	1.22*	0.876(9)	4
O1	0.1767(5)	0.1683(5)	0.0489(4)	2.81*	0.913(14)	4
O2	0.0537(6)	0.5842(7)	0.2171(7)	5.19*	0.769(15)	4
O3	0.6276(5)	0.9898(7)	0.1763(5)	2.43*	0.796(13)	4
O4	0.6497(6)	0.5173(6)	0.1348(4)	3.19*	0.816(14)	4
	U_{11}	U_{22}	U_{33}	U_{12}	U_{13}	U_{23}
Ce1	5.46(32)	7.3(4)	2.51(24)	2.41(28)	0.84(18)	0.75(25)
Ta1	1.02(15)	1.42(16)	1.23(17)	0.17(14)	0.33(11)	−0.91(13)
O1	3.64(25)	4.59(29)	0.36(20)	1.09(18)	0.44(14)	0.60(14)
O2	3.28(37)	3.18(32)	9.71(51)	5.14(25)	3.46(32)	4.98(26)
O3	4.10(34)	0.35(25)	3.10(28)	1.63(18)	1.25(20)	0.46(17)
O4	7.56(40)	0.69(25)	1.30(27)	−2.15(21)	0.23(22)	1.03(16)

$R_p = 4.69\%$, $R_{wp} = 5.56\%$, $\chi^2 = 1.873$.

Table 7
Calculated bond distances for $CeTaO_{4+\delta}$ in air at 800°C

Bond	Length (Å)	Bond	Length (Å)
Ce–O1	2.550(5)	Ta–O1	1.988(4)
Ce–O2	2.850(5)		2.000(4)
Ce–O3	2.419(6)	Ta–O2	2.062(5)
	2.350(6)		1.902(5)
	2.519(6)	Ta–O3	2.049(5)
Ce–O4	2.502(5)	Ta–O4	1.925(5)
	2.656(6)		
	2.398(5)		

reduction in the oxygen stoichiometry and also indicated a slight Ce:Ta non-stoichiometry (Table 6). From this it would be reasonable to conclude that there had been some exsolution of CeO_2, as found in the samples heated under vacuum conditions.

Previous reports [2,3] have indicated that the structural chemistry of $CeTaO_{4+\delta}$ involves several phases, with the $CeTaO_{4.17}$ phase being a superstructure corresponding to a stoichiometry of $Ce_6Ta_6O_{25}$. In this case the data were refined to the "subcell" $CeTaO_{4.17}$ with typical lattice parameters being $a = 7.69233(6)$ Å, $b = 5.55517(5)$ Å, $c = 7.75548(4)$ Å and $\beta = 102.976(1)^\circ$ at 800°C. There was no evidence from the powder neutron diffraction data at any temperature of superstructure peaks and therefore there was no justification for fitting to the superstructure model, despite the structural refinement from X-ray diffraction data proposed by Thomson et al. [2].

Bond distances calculated from this refinement are presented in Table 7 and show that the overall Ce coordination environment is reduced to eight-fold when compared to the orthorhombic model presented earlier. It is also evident that the distances, 2.350–2.850 Å are significantly shorter than in the orthorhombic model whereas the Ta–O coordination environment remains largely unchanged.

4. Conclusions

From this work it was found that an orthorhombic $A2_1am$ phase exists at a temperature of 900°C and therefore the anticipated structure of the high temperature modification of $CeTaO_4$ is indeed isostructural with the high temperature modification of $LaTaO_4$. However it was also found that $CeTaO_4$ decomposed readily leaving a slight Ce deficiency and excess CeO_2 when examined under vacuum conditions. It was also determined that the orthorhombic modification could not be produced on heating $CeTaO_{4.17}$ in air, with the monoclinic phase existing at all temperatures examined.

Acknowledgments

We would like to acknowledge the support of the EPSRC in funding this work through ROPA grant reference GR/R23374/01 and the CCLRC for the award of the neutron diffraction beam time, RB13194. Further thanks are due to Dr. Richard Ibberson, RAL, for his assistance in operating the HRPD instrument.

References

[1] S.J. Skinner, Solid State Ion. 154–155 (2002) 325.
[2] J.G. Thomson, A. David Rae, N. Bliznyuk, R.L. Withers, J. Solid State Chem. 144 (1999) 240.
[3] G. Drew, R.L. Withers, A.-K. Larsson, S. Schmid, J. Solid State Chem. 140 (1998) 20.
[4] A. Santoro, M. Marezio, R.S. Roth, D. Minor, J. Solid State Chem. 35 (1980) 167.
[5] R.S. Roth, T. Negas, H.S. Parker, D.B. Minor, C.D. Olson, C. Skarda, in: G.J. McCarthy, J.J. Rhyne (Eds.), The Rare Earths in Modern Science and Technology, Plenum Press, New York, London, p. 163.
[6] R.S. Roth, T. Negas, H.S. Parker, D.B. Minor, C. Jones, Mater. Res. Bull. 12 (1977) 1173.
[7] T. Negas, R.S. Roth, C.L. McDaniel, H.S. Parker, C.D. Olson, Mater. Res. Bull. 12 (1977) 1161.
[8] R.J. Cava, T. Negas, R.S. Roth, H.S. Parker, D.B. Minor, C.D. Olson, in: G.J. McCarthy, J.J. Rhyne (Eds.), The Rare Earths in Modern Science and Technology, Plenum Press, New York, London, p. 181.
[9] R.J. Cava, R.S. Roth, J. Solid State Chem. 36 (1981) 139.
[10] T. Esaka, R. Tachibana, S. Takai, Solid State Ion. 92 (1996) 129.
[11] S. Takai, S. Touda, K. Oikawa, K. Mori, S. Torii, T. Kamiyama, T. Esaka, Solid State Ion. 148 (2002) 123.
[12] H.W. Huang, Z.G. Ye, M. Dong, W.L. Zhu, X.Q. Feng, Jpn. J. Appl. Phys. 41 (6B) (2002) L713.
[13] G.G. Zhang, Q.F. Fang, X.P. Wang, Z.G. Yi, J. Phys.: Condens. Matter 15 (2003) 4135.
[14] H. Huang, X. Feng, Z. Man, T.B. Tang, M. Dong, Z.G. Ye, J. Appl. Phys. 93 (2003) 421.
[15] E.V. Tsipis, V.V. Kharton, N.P. Vyshatko, A.L. Shaula, J.R. Frade, J. Solid State Chem. 176 (2003) 47.
[16] S.J. Skinner, Y. Kang, Solid State Sci. 5 (2003) 1475.
[17] R. von Dreele, A. Larson (Eds.), General Structural and Analytical Software, Los Alamos National Laboratory, USA, 2001.